Journal of Materials Chemistry A

Accepted Manuscript

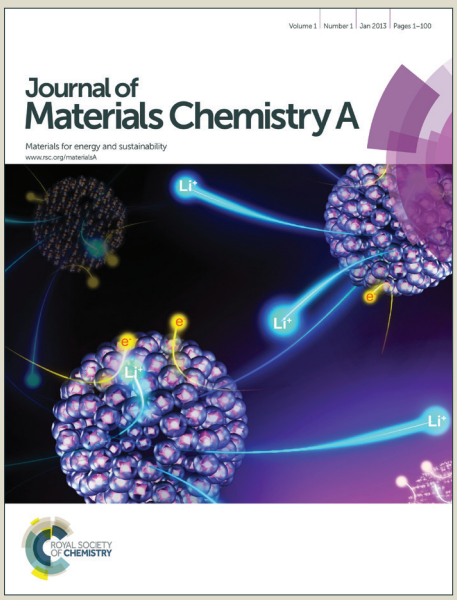

ROYAL SOCIETY OF CHEMISTRY

www.rsc.org/materialsA

Cite this: DOI: 10.1039/c0xx00000x

www.rsc.org/xxxxxx

PAPER

Preparation of MWCNTs grafted with polyvinyl alcohol through Friedel-Crafts alkylation and their composite fibers with enhanced mechanical properties

Pei Zhang, Dianluan Qiu, Hongfei Chen, Jun Sun, Jianjun Wang, Chuanxiang Qin, Lixing Dai*

Received (in XXX, XXX) Xth XXXXXXXXX 20XX, Accepted Xth XXXXXXXXX 20XX
DOI: 10.1039/b000000x

An effective method to increase mechanical properties of poly (vinyl alcohol) (PVA) and multi-walled carbon nanotubes (MWCNTs) composite fibers is reported. MWCNTs in the composite fibers were functionalized with PVA through one-step grafting process by nondestructive Friedel-Crafts alkylation in an aluminum chloride medium. Under suitable conditions, the resulting functionalized MWCNTs (f-MWCNTs) of selected content of 0.05 wt% based on PVA weight was added to DMSO/H_2O (vol ratio=3/1) mixed solvent, and f-MWCNTs were highly dispersed in the solution, which remained uniform even after stayed 30 days. The solution was gel spun and the as-spun fibers were hot drawn to prepare the final PVA/f-MWCNTs composite fibers. The tensile strength and modulus of the fibers were found to be about 926 MPa and 59 GPa which increased by 280.6% and 421.0% relative to pure PVA fibers, respectively.

1. Introduction

It is an important way to fabricate high-strength fibers through filling the polymer matrix with materials of excellent mechanical properties in recent years.[1-3] Carbon nanotube (CNT), a one-dimensional material, has outstanding mechanical properties such as extreme tensile strength and impressive Young's modulus,[4-7] which make it ideal filler to achieve high strength polymer composite.[8, 9] Significant efforts have been made in the fabrication of these composites by dispersing CNT into various polymer matrices to prepare composites of interesting properties. However, the strength of CNT composites are far from that we expected. The critical challenges are the aggregation of CNT and the poor stress transfer mechanism between CNT and the polymer matrix,[10] reducing the reinforcing effect to a large extent. So the key points to successful improvement of the CNT composite performance are dispersion of CNT and enhancement of interfacial bonding between CNT and polymer matrix. It has been proved to be effective in the literature[11] that the materials functionalized with a defined structure have good chemical affinity with the polymer matrix, and can be used as active fillers in composite to obtain excellent performance.

Polyvinyl alcohol (PVA), a typical polyhydric alcohol containing a large number of hydroxyl groups in molecular chain, has been considered as a suitable matrix for CNT composites.[11-13] In recent years, several studies have focused on composites made of PVA loaded with CNT, including two main routes, non-covalent adsorption and covalent sidewall grafting. Non-covalent adsorption is mainly dependent on the Vander Waals force or π-π interactions between CNT and PVA matrix.[14, 15] Vigolo *et al.*[16] employed a method to disperse the CNT in surfactant solutions, i.e. recondensed the CNT in the flow of a PVA solution to form long ribbons and fibers. Uddin *et al.*[17] achieved good dispersion of the SWCNTs in an organic solvent and finally high-performance composite fibers using green tea extract as a dispersant to stabilize SWCNTs in PVA solution. Mercader *et al.*[12] reported a water-based spinning process to produce PVA/CNT composite fibers that contained a large fraction of nanotubes with the addition of SDS. The common problems of these non-covalent methods are unstable interfacial bond of CNT with polymer matrix and restriction of strength enhancement of the CNT composites. On the other hand, the most popular method of covalent modification first reported by Liu *et al.*[18] is treating CNT in acid to bring oxidized groups to its surface. Strong electrostatic repulsion between the acidified CNTs forces them to disperse uniformly in the solution, which helps them to intimately mix with polymer matrix.[19] In addition, these oxygen-containing functional groups (predominantly carboxyl) induced by oxidation can then be used as chemical anchors for further covalent modification through esterification or amidation reactions.[20] Lin. *et al.*[21] prepared nanocomposite films of CNT/PVA by the esterification reaction. However, the CNTs were terribly shortened which restricted the strength enhancement of the CNT composites and the process is also too complicated to achieve commercially available.

Therefore, a new method is expected to be found to disperse CNT well, but have little or no structure damage to CNT. Friedel-Crafts alkylation (FC alkylation) is a special class of electrophilic aromatic substitution in which the electrophile is a carbocation, and it has been successfully applied for the chemical functionalization of CNT with small molecules[22-24]. The approach

is more feasible than the traditional carboxylation because the surface modification of CNT with functional groups is not needed before the grafting of macromolecules to CNT. Moreover, as acidic treatment process for CNT, those oxided by the mixed acid are mainly metastable carbon atoms in five-membered rings and seven-membered rings. Such strong acidification forces the walls of CNT to break and peel off, left severe destruction of the graphitic structure of CNT.[25] However, in FC alkylation it is the benzene rings on the sidewall of CNT that participate the reaction, thus the reaction sites are far more adequate than the acidic treatment, and the attacking of carbocations does not damage the CNT surface. So the alkylation is a less destructive or nondestructive reaction for efficient dispersion and functionalization of CNT.[26] Kumar *et al.*[24] reported an effective route to prepare highly conducting and flexible few-walled carbon nanotube (FWNT) thin films. The free-standing thin films were fabricated by functionalizing FWNTs with 4-ethoxybenzoic acid (EBA) via a direct FC acylation reaction in a nondestructive medium. Wu *et al.*[26] developed a novel approach for the surface modification of MWCNTs with high percentage of grafting of poly(vinyl chloride) (PVC) via the FC acylation. However the grafting of PVA with CNT through one-step grafting process by FC alkylation and the fabrication of the composite fibers has not been reported.

In this work, the grafting of PVA onto MWCNTs via one-step grafting process by FC alkylation reaction with anhydrous aluminum chloride ($AlCl_3$) as catalyst was carried out. The one-step process does not need first form a CNT intermediate before polymer molecules bond to CNT as traditional process. Dispersion of the functionalized MWCNTs (f-MWCNTs) in PVA solution and the properties of the PVA/f-MWCNTs composite fibers were discussed.

2. Experimental procedure

2.1 Materials

PVA (degree of polymerization 1750, alcoholysis degree 98%, M_w=74800), Dimethyl sulfoxide (DMSO) and aluminum chloride (AR) were purchased from Sinopharm Chemical Reagent Co., Ltd (China). MWCNTs (20-30nm outer diameter and 10-30μm length) were purchased from Chengdu Organic Chemicals Co., Ltd. (China).

2.2 Preparation of grafted MWCNTs with PVA by FC alkylation

MWCNTs (0.2 g), PVA (2 g), and DMSO (20 ml) were placed into a three-necked flask equipped with a magnetic stirrer, nitrogen inlet and outlet and immersed in an oil bath. The mixture in the flask was slowly heated from room temperature to 90 ^oC under stirring, and when the PVA was completely dissolved, 1g aluminum chloride ($AlCl_3$) as a catalyst was added. The mixture was continually stirred at 70 ℃ for 24h under nitrogen atmosphere. The reaction was terminated by pouring the mixture into methanol/hydrochloric acid (vol ratio=1/1), then centrifuged at 3000 rpm for 15 min and washed the precipitates with distilled water several times until no $AlCl_3$ could be detected, finally the f-MWCNTs were obtained after dried at 70 ^oC for 3h. As a contrast,

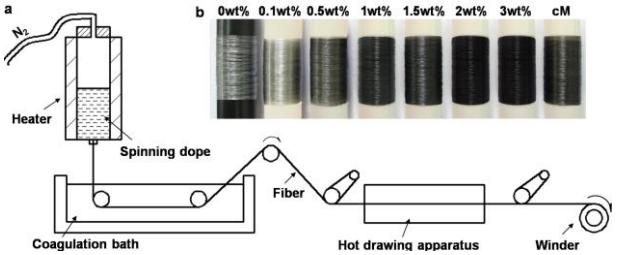

Fig. 1 (a) Spinning apparatus for preparing PVA/f-MWCNTs composite fibers. (b) Photograph of the composite fibers with different f-MWCNTs loadings (marked on the tops) and cM represents the composite fiber with 0.5 wt% c-MWCNT loading.

carboxyl group functionalized MWCNTs (c-MWCNTs) were prepared through oxidizing MWCNTs in concentrated sulfuric and nitric acid (vol ratio=3/1) at 70 ℃ for 24h according to the process reported in the literature.[27]

2.3 Preparation of PVA/f-MWCNTs composite fibers

f-MWCNTs were dispersed in DMSO/H_2O mixed solvent (vol ratio=3/1) and a 30 min bath-sonication in water was carried out to ensure homogenous dispersion using a sonication equipment KQ118 (40kHz, output power 70W) produced by Kunshan Sonication Equipment Co. Ltd., China. Then a certain amount of f-MWCNTs dispersion was added into 14 wt% PVA solution (the same solvent composition as f-MWCNTs dispersion) to prepare a series of spinning dope with different f-MWCNTs contents. Composite fibers were fabricated by wet spinning with a self-made spinning apparatus, coagulating in methanol at 0 ^oC, and drawing at a ratio of 12 (Fig. 1a). Then a set of fibers with MWCNT mass fractions of 0, 0.1, 0.5, 1, 1.5, 2, and 3 wt% to PVA weight were obtained. Under the same conditions, c-MWCNTs were dispersed in the same mixed solvent as f-MWCNTs and composite fibers of PVA/c-MWCNTs (0.5 wt% to PVA weight) were prepared (Fig. 1b).

2.4 Characterization

Raman spectra were obtained on a HR800 Raman Microscope equipped with a laser diode source emitting at 514 nm. UV transmission spectra of MWCNTs dispersions were measured via a Varian CARY50 Ultraviolet-visible (UV-vis) spectrometer. The dispersion of MWCNTs was observed by TecnaiG220 transmission electron microscopy (TEM). Scanning electron microscopy (SEM) images were taken on a Hitachi S–4700 field-emission SEM system. Solid state NMR measurements were performed on a Bruker Avance III 400 spectrometer operating at a Larmor frequency of 100.64 MHz for ^{13}C, and equipped with a double-resonance magic-angle spinning (MAS) probe, supporting MAS rotors of 3.2 mm outer diameter. Thermal gravimetric analysis (TGA) was carried out on a Perkin-Elmer Pyris 6 TGA instrument with a heating rate of 10^oC min^{-1} under nitrogen flow. Differential scanning calorimetric (DSC) analysis was performed on Mettler TA Q200 equipment. The melting temperature (T_m) and degree of crystalline (X_c) were determined based on DSC curves. Mechanical properties of the fibers were measured by an HD021N fiber strength instrument with gauge length 10cm and a crosshead speed 20 mm min^{-1}, and the experimental results were evaluated as the averages of at least five measurements.

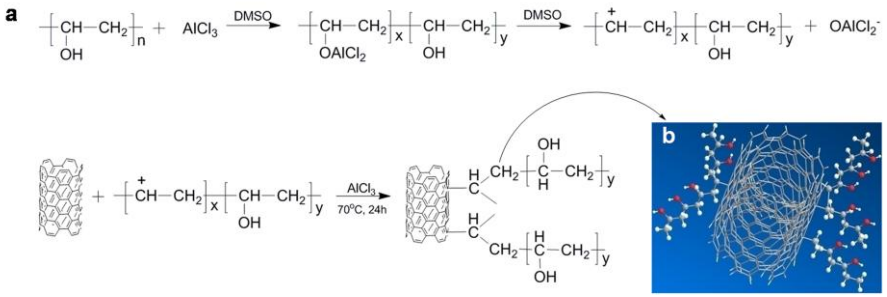

Fig. 2 (a) Functionalization of MWCNTs with PVA by FC alkylation reaction, (b) cartoon depicting of f-MWCNTs structure.

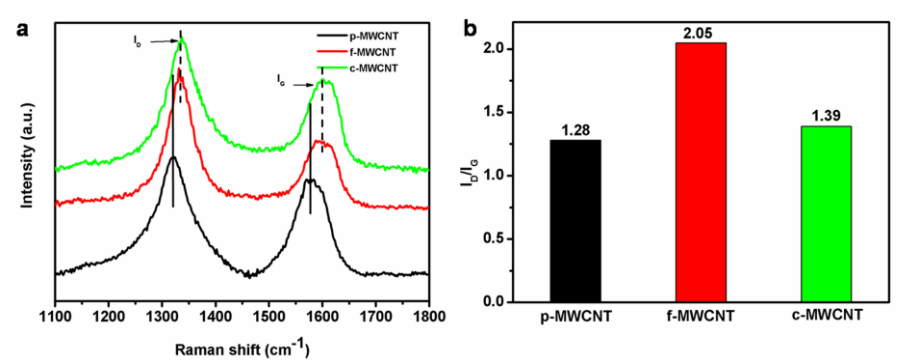

Fig. 3 Raman characterization of p-MWCNTs, c-MWCNTs and f-MWCNTs via FC alkylation: (a) Raman spectra. (b) Intensity ratio of I_D/I_G

3. Results and Discussion

In the experimental procedures of the grafting with PVA to MWCNTs, $AlCl_3$ combines with the hydroxyl on PVA backbones and is then split off, forming carbocations and aluminum compound anions. Carbocations then attack the benzene ring on the MWCNTs surface due to their inherent eletrophilicity. Subsequently the PVA chains are grafted to the surface of MWCNTs, that is, f-MWCNTs are obtained as depicted in Fig. 2.

The Raman spectrum of pristine MWCNTs (p-MWCNTs), f-MWCNTs, and c-MWCNTs are shown in Fig. 3. Two usual bands were detected for the MWCNTs: The G-band near 1590 cm^{-1} corresponds to the Raman-active E_{2g} mode of graphite due to *sp2* hybridized carbons while the D-band around 1350 cm^{-1} is attributed to either *sp3* hybridized carbons or structural defect sites of the *sp2* hybridized carbon network.[28] By determining the ratio between these two bands (I_D/I_G), a quantitative measure of defect density in the CNT sidewall can be ensured. Consequently, I_D/I_G band analysis can be used to obtain information regarding structural changes as a result of functionalization such as the attachment of organic moieties.[29] I_D/I_G of p-MWCNTs is about 1.28, while I_D/I_G is around 2.05 for f-MWCNTs as shown in Fig. 3b, which is because that when PVA is grafted to the surface of MWCNTs via FC alkylation, more *sp3*-hybridized carbons of the nanotube sidewalls were produced, disrupting their regular graphitic structure,[26] which undoubtedly affect I_D/I_G and the peak positions in Raman spectrum. While the intensity ratio of c-MWCNTs is 1.39, which is mainly due to intercalation of acid molecules, exerting pressure on the *sp*2 structure, an electron transfer from the π states in MWCNTs to the oxygen atoms and the structural defect sites of the *sp2* hybridized carbon network.[30] We'll further demonstrate it in the following TEM

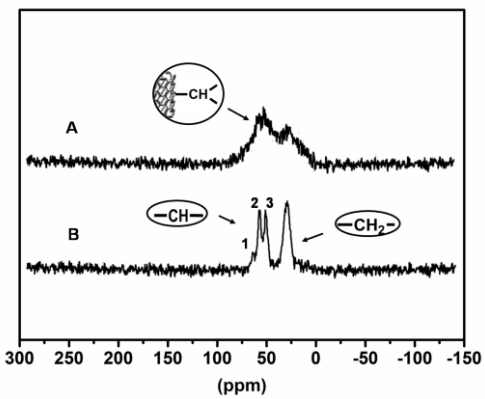

Fig. 4 ^{13}C CP/MAS spectra of: (A) f-MWCNTs, (B) pure PVA.

characterization. Besides, the D-band and G-band of the modified MWCNTs, both f-MWCNTs and c-MWCNTs, shift to higher frequencies by 13 and 22 cm^{-1} respectively than the peak of p-MWCNTs as shown in Fig. 3a, which can be explained by the disentanglement of the MWCNTs and a consequence of strong compressive forces associated with surface groups on MWCNTs.[31] This clearly indicates that PVA chains were covalently bonded on the surface of the MWCNTs after FC alkylation. Similar up-shifting of the D-band and G-band has been reported for SWCNTs reinforced epoxy resins[32] and polypropylene[33].

Solid state ^{13}C NMR was used to demonstrate that whether PVA chains were chemically bonded with MWCNTs during the FC alkylation reaction (Fig. 4). Measurements were carried out at room temperature, rf-nutation frequencies for ^{1}H and ^{13}C were 78 kHz, corresponding to 3.2 μs for 90° pulse. 1D ^{13}C cross polarization/magic-angle spinning (CP/MAS) spectra were

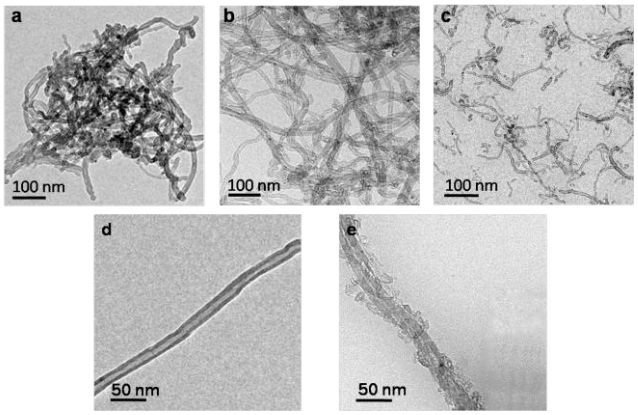

Fig. 5 TEM images of (a) p-MWCNTs, (b) f-MWCNTs and (c) c-MWCNTs. (d) single p-MWCNTs and (e) single f-MWCNTs in DMSO/H_2O (vol ratio = 3/1).

accumulated with a CP contact time of 0.5 ms, a recycle delay of 5 s, and SPINAL-64 as heteronuclear decoupling technique applied during acquisition. Fig. 4 is the ^{13}C CP/MAS NMR spectra of f-MWCNTs and pure PVA, peaks at 37 ppm correspond to -CH_2- of PVA chain, while the peaks between 50-60 ppm are ascribed to -CH- group. In the ^{13}C CP/MAS NMR spectrum of PVA in the solid state, the ^{13}C signal for the -CH- carbon with three splitting peaks is observed as shown in Fig. 4B. Such a splitting is caused by the number of intramolecular hydrogen bonds with neighbouring hydroxyl groups. Peak 1, peak 2, and peak 3 come from the -CH- carbons forming two hydrogen bonds, one hydrogen bond, and no hydrogen bonds with the hydroxyl group, respectively.[34] Although the positions of peaks in the two spectra are generally similar, the peaks in f-MWCNTs are more broadened than in pure PVA, and the peak tenacity of -CH- also succeeds that of -CH_2-, which may be due to the paramagnetic nature of carbon nanotubes.[35] Moreover, peak 1 and peak 2 of -CH- of the f-MWCNTs are almost disappeared, indicating that an amount of hydroxyl groups on PVA chain have reacted with the benzene ring on the surface of MWCNTs. Similar phenomenon has been observed and reported for other polymer functionalized carbon nanotubes.[36-38]

Fig. 5 shows TEM images of p-MWCNTs, f-MWCNTs and c-MWCNTs in DMSO/H_2O. p-MWCNTs display a strong trend to aggregate (Fig. 5a), while f-MWCNTs after FC alkylation are homogeneously dispersed in the solution and show no obvious destructive structural damage (Fig. 5b). In contrast, unlike f-MWCNTs, after oxidation, some bundles appear exfoliated and curled, severe fragmentation of the MWCNT structure takes place as clearly indicated in Fig. 5c. Thus, the treatment of MWCNTs with strong oxidizing agents causes severe etching of the graphitic surface of MWCNT, leading to tubes of shorter length with a large population of disordered sites. Fig. 5d and 5e are images of single p-MWCNT tube and single f-MWCNT tube, respectively, which clearly show that the surface of the p-MWCNT is clean and smooth with nothing adhering, while the surface of f-MWCNT is wrapped with molecular chains, indicating PVA chains were effectively grafted to the MWCNT surface through FC alkylation.

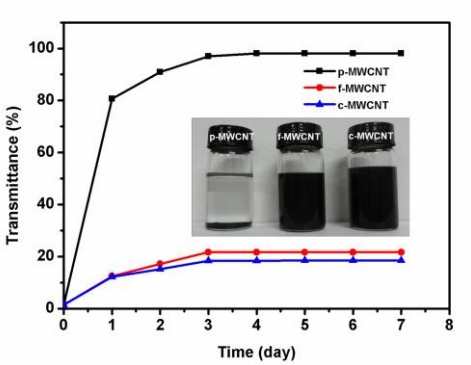

Fig. 6 UV−vis transmittances of p-MWCNTs, f-MWCNTs and c-MWCNTs. The content of MWCNT is 0.05 wt%. Inset: image of the dispersed samples after 7 days.

The dried p-MWCNTs, f-MWCNTs and c-MWCNTs with the same concentration (0.05 wt%) were dispersed into DMSO/H_2O mixed solvent (vol ratio=3/1) with stirring for 20 min and then left free-standing for 1 week. Based on the *sp2* structure of CNT, UV detector was used to measure the transmittance of MWCNTs in the supernatant, which reflects the dispersity of the MWCNTs, that is, the higher the transmittance, the worse the dispersity.

The UV−vis spectra of each sample after storage for different periods were recorded as shown in Fig. 6. For p-MWCNTs, most of MWCNTs are deposited in first day and the transmittance is almost 100% after the first three days, indicating that the MWCNTs deposited relatively rapidly. However the transmittance of modified MWCNTs, whatever f-MWCNTs or c-MWCNTs, increase only about 12% in the first day and keep stable in the following several days, proving their good dispersion intuitively. After one week storage, the visualized results were obtained by camera as shown in the inset of Fig. 6. The picture corresponding to the transmittances provides much intuitive evidences for the dispersibility of p-MWCNTs and modified MWCNTs dispersed in the mixed solvent. It shows that the p-MWCNTs have poor dispersion in the solvent, whereas the solutions of the f-MWCNTs and c-MWCNTs exhibit homogeneous dispersion and scarcely any sedimentation was observed. Apparently, it is because the introduction of hydroxyl in PVA to the surface of MWCNTs via FC alkylation which causes the f-MWCNT to show good dispersion. Besides, due to the fact that the side walls of the c-MWCNTs carry more dissociated carboxyl groups after oxidization with the acid mixture, the nanotubes can stabilize via an electrostatic stabilization mechanism.[39]

In order to determine the thermal stability of f-MWCNT and the role of f-MWCNTs in melting and crystallization behaviour of PVA/f-MWCNTs composite fibers, TG and DSC thermal analysis have been performed.

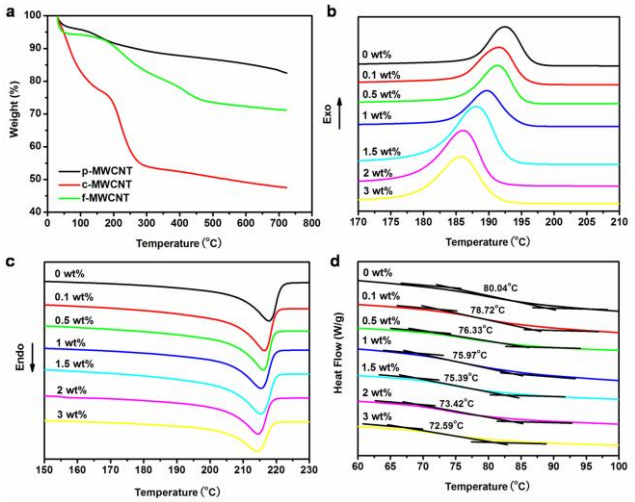

Fig. 7 (a) TG curves of p-MWCNTs, c-MWCNTs and f-MWCNTs. DSC curves of PVA/f-MWCNTs composite fibers: (b) cooling curves, (c) (d) heating curves with different f-MWCNTs loading marked on each curve.

Table1 Thermal properties and crystallinity (X_c) of PVA/f-MWCNTs composite fibers.

MWCNT content (wt%)	T_m (°C)	T_c (°C)	ΔH_m (J/g)	X_c (%)
0	217.91	192.46	43.61	31.46
0.1	216.37	191.48	40.63	29.31
0.5	216.04	191.36	38.96	28.11
1	215.48	189.74	37.39	26.98
1.5	215,41	187.98	36.75	26.52
2	214.56	186.06	35.33	25.49
3	214.41	185.76	33.57	24.22

As shown in Fig. 7a, the comparisons of thermal stability of p-MWCNTs, f-MWCNTs and c-MWCNTs were made. p-MWCNTs are the most stable among the three samples and do not show dramatic decomposition in the temperature range of 50-700 °C. It is clear that the thermal degradation of f-MWCNTs exceeds p-MWCNTs from 200 to 400 °C, which is mainly attributed to decomposition of PVA chains wrapped on MWCNTs.[40] c-MWCNTs lose their weight drastically from 50 to 250 °C and weight loss is the largest at the same temperature, near 35% more than f-MWCNTs, which is caused by the decomposition of oxidation group on the surface of MWCNTs induced by acidification. Obviously, the thermal stability of f-MWCNTs is much better than c-MWCNTs.

The DSC cooling curves and heating curves of PVA/f-MWCNTs composite fibers are shown in Fig. 7b, 7c, and 7d and the data are summarized in Table 1. The specimens were first heated from room temperature to 250 °C at a heating rate of 10 °C min^{-1} and kept for 10 min to erase the thermal history. The crystallization behaviors, i.e. cooling curves, were recorded from 250 °C to 40 °C at cooling rates of 10 °C min^{-1} and kept for 2 min at 40°C. And then the specimens were second heated from 40 to 250 °C at a heating rate of 10° C min^{-1} to obtain heating curves. It can be seen from Fig. 7b that all the composites have only one exothermic peak, and the crystallization temperature (T_c) gradually decrease from 192.46 °C to 185.76 °C with the increase of the amount of f-MWCNTs from 0 to 3 wt%. And increasing amount of f-MWCNTs also leads to decreasing melting

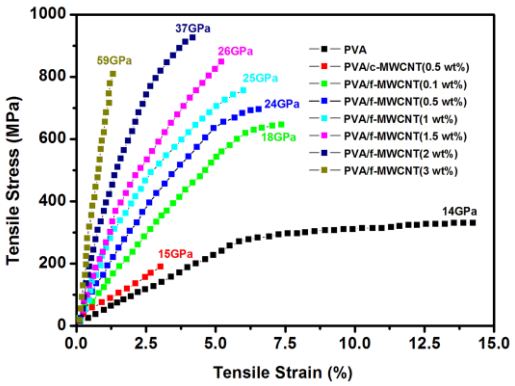

Fig. 8 Stress-strain curves of PVA/f-MWCNTs composite fibers, the values on the tips of curves are Young's modulus of the corresponding fibers.

temperature (T_m) of PVA/f-MWCNTs composites (from 217.91 to 214.41 °C). A lower T_c indicates thinner lamellae or disorder arrangement of lamellae,[41] which is probably because the existence of MWCNTs limits the movement of the PVA chain, reducing the probability of the chain to arrange regularly in the lattice. Glass transition temperatures (T_g) of PVA/f-MWCNTs composite fibers as shown in Fig. 7d, decrease from 80.4 to 72.59 °C corresponding to the loading of f-MWCNTs increasing from 0 to 3 wt%. The result infers that the intermolecular and inner molecular hydrogen bonds of PVA are weakened in the PVA/f-MWCNTs composite fibers, indicating a certain amount of hydroxyl groups reacted with MWCNTs via FC alkylation, moreover, well dispersed MWCNTs could hinder the formation of hydrogen bonds due to their large bulk in the composites.

Melting enthalpy (ΔH_m) and crystalline degree (X_c) were also determined from the heating scan. X_c of PVA in the composite fibers was calculated as follows:

$$X_C = \frac{\Delta H_m}{w\Delta H_O}$$

where ΔH_m is measured from DSC and ΔH_0 is the enthalpy of pure PVA crystal (138.6 J g^{-1}).[42] As shown in Table 1, obvious gradual reduction of PVA crystallinity is observed in PVA/f-MWCNTs composites containing from 0 to 3 wt% f-MWCNT.

The stress-strain curves for the composite fibers are shown in Fig. 8. In this case, the samples were at least measured for five times and the average values are taken. The result reveals that PVA/f-MWCNTs composite fibers acquire a pronounced improvement in mechanical properties. The tensile strength of the fibers increased from 330 to 926 MPa corresponding to the amount of f-MWCNTs from 0 to 2 wt%, but as f-MWCNTs loading is up to 3 wt%, the strength decreases to 805 MPa instead, which suggests the agglomerates of f-MWCNTs in the composite fibers. The Young's modulus increases linearly from 14 GPa for pure PVA to 59 GPa for PVA/f-MWCNTs (3 wt%) fiber. The degree of crystallinity decreases, but the strength and modulus are still improved, which is probably because the enhancing effect of MWCNT exceeds the impact of the decline of crystallization. It is noteworthy that when the loading of f-MWCNTs are 0.5 wt%, the strength and modulus of PVA/f-MWCNTs composite fiber are about 695 MPa and 24 GPa, 265% and 60% higher than that of PVA/c-MWCNTs composite fiber with the same c-MWCNTs loading (0.5 wt%), respectively. Moreover, even a very small

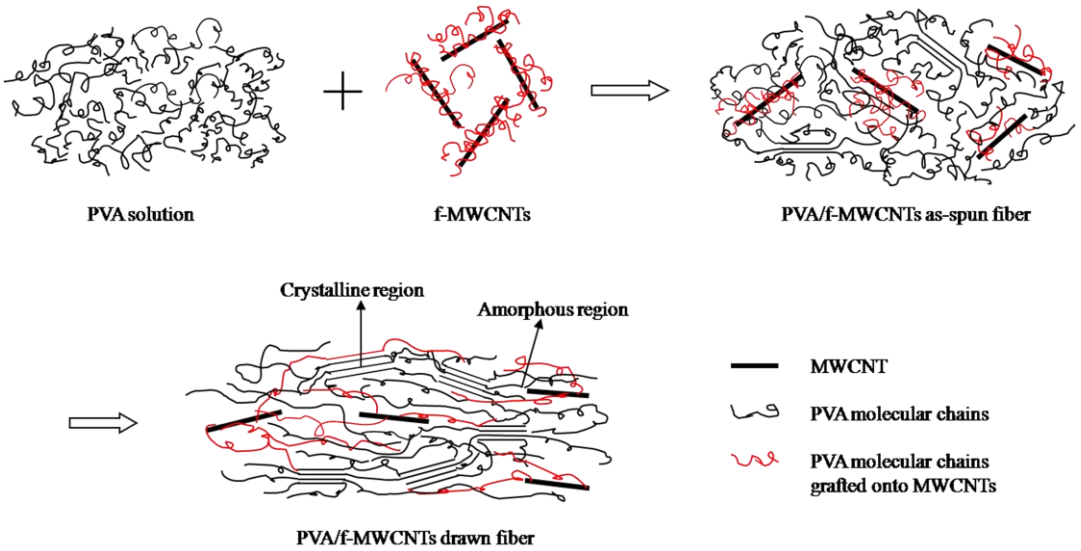

Fig. 9 Proposed structural model of PVA/f-MWCNTs composites fibers.

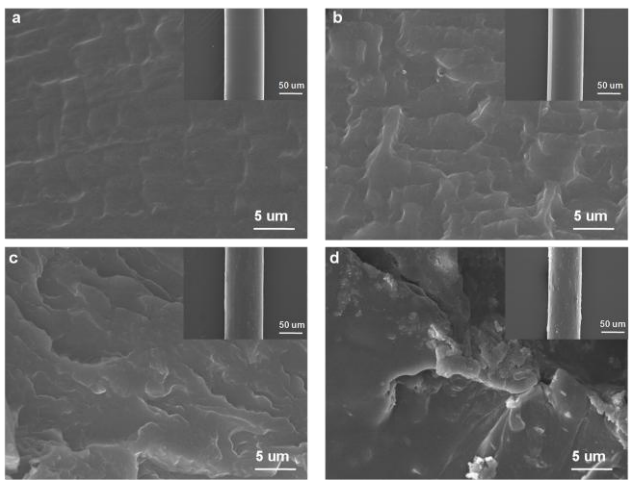

Fig. 10 Selected SEM images of cross-sections of PVA/f-MWCNTs composite fibers containing different amount of f-MWCNTs: (a) 0 wt%, (b) 1 wt%, (c) 2 wt%, (d) 3 wt%. Insets: the surface morphology of the corresponding fibers.

amount of f-MWCNTs (0.1 wt%) dopes in the composite fiber, the strength of the fiber is still twice higher than that of PVA/c-MWCNTs(0.5wt%) fiber. It is clear that for functionalization of MWCNT, FC acylation is more feasible and effective than acidic treatment.

The structure model of PVA/f-MWCNTs composite fibers is shown in Fig. 9. Undoubtedly, f-MWCNTs are well compatible with PVA, and uniformly disperse in PVA matrix at the suitable amount of f-MWCNTs. When the as-spun composite fibers are drawn, the molecular chains of the PVA matrix and the chains of PVA grafted to MWCNTs are oriented, resulting in strengthening their interfacial bonding, which will increase the load transferring from PVA matrix to f-MWCNTs. In addition, the drawing facilitates growth and orientation of crystalline, which also has positive effect on the increase of mechanical behavior of the PVA/f-MWCNTs composite fibers.

Fig. 10 is SEM images of cross-sections and surfaces of the composite fibers and the cross sections were prepared by cutting the fibers in liquid nitrogen to give an intact surface fracture. The insets in Fig. 10 are the images of the fiber surfaces in longitudinal direction. The cross sections of the composite fibers become gradually rough with f-MWCNTs loading from 0 to 3 wt%, which may result from the gradually strengthening f-MWCNT-polymer interaction.[43] The fibers with f-MWCNTs amount of 1 and 2 wt% present a relatively uniform morphology, while the composite fiber containing 3 wt% f-MWCNTs is quite different, and the cross section seems uneven, which should be due to the aggregation of the f-MWCNTs. As shown in the insets in Fig. 10, the surface of pure PVA fiber is smooth and homogenous. The composite fibers, containing f-MWCNTs of 1 and 2 wt%, display few MWCNT clusters in the surfaces, and clearly show that the f-MWCNTs are homogeneously dispersed in the PVA without aggregation at a low f-MWCNT concentration. However, when the MWCNT loading increases to 3 wt%, small projections and particulates appear on the surface, limiting the reinforcement of the composite fibers, which is in good agreement with Fig. 8.

4. Conclusions

On the basis of characterization results, PVA was effectively grafted onto the surface of MWCNTs, and the resulting f-MWCNTs showed improved uniformity and good dispersion in DMSO/H_2O mixed solvent. Then the f-MWCNTs were dispersed in PVA solution to prepare spinning dope, continuous PVA/f-MWCNTs composite fibers were fabricated using wet-spinning process. The composite fibers were much stronger and stiffer than either those prepared from pure PVA or mixtures of c-MWCNT and PVA, indicating the efficient load transferring of f-MWCNTs from PVA matrix, thus acquirement of high strength PVA/f-MWCNTs composite fibers.

Acknowledgments

This research was supported by Natural Science Fund of Jiangsu Province (BK2012623) and A Project Funded by the Priority Academic Program Development of Jiangsu Higher Education Institutions.

Notes and references

* *College of Chemistry, Chemical Engineering and Materials Science, Soochow University, Suzhou, Jiangsu, 215123, People's Republic of China. Fax: +86-0512-65880906; Tel: +86-0512-65880906 Email address: dailixing@suda.edu.cn*

1. R. Sengupta, M. Bhattacharya, S. Bandyopadhyay and A. K. Bhowmick, *Progress in Polymer Science*, 2011, **36**, 638.
2. Z. Spitalsky, D. Tasis, K. Papagelis and C. Galiotis, *Progress in Polymer Science*, 2010, **35**, 357.
3. A. Patnaik, A. Satapathy, N. Chand, N. Barkoula and S. Biswas, *Wear*, 2010, **268**, 249.
4. J. Salvetat, J. Bonard, N. Thomson, A. Kulik, L. Forro, W. Benoit and L. Zuppiroli, *Applied Physics A*, 1999, **69**, 255.
5. J. P. Salvetat Delmotte and A. Rubio, *Carbon*, 2002, **40**, 1729.
6. B. I. Yakobson and P. Avouris, in *Carbon nanotubes*, Springer, 2001, **pp**. 287.
7. M. Sammalkorpi, A. Krasheninnikov, A. Kuronen, K. Nordlund and K. Kaski, *Physical Review B*, 2004, **70**, 245416.
8. X. Wang, Q. Jiang, W. Xu, W. Cai, Y. Inoue and Y. Zhu, *Carbon*, 2013, **53**, 145.
9. Q. Song, K. Li, H. Li, H. Li and C. Ren, *Carbon*, 2012, **50**, 3949.
10. X. Xie, Y. Mai and X. Zhou, *Materials Science and Engineering: R: Reports*, 2005, **49**, 89.
11. X. Xu, A. J. Uddin, K. Aoki, Y. Gotoh, T. Saito and M. Yumura, *Carbon*, 2010, **48**, 1977.
12. C. Mercader, V. D. Lutard, S. Jestin, M. Maugey, A. Derré, C. Zakri and P. Poulin, *Journal of Applied Polymer Science*, 2012, **125**, E191.
13. G. Park, Y. Jung, G. W. Lee, J. P. Hinestroza and Y. Jeong, *Fibers and Polymers*, 2012, **13**, 874.
14. C. Bartholome, P. Miaudet, A. Derré, M. Maugey, O. Roubeau, C. Zakri and P. Poulin, *Composites Science and Technology*, 2008, **68**, 2568.
15. L. Lu, W. Hou, J. Sun, J. Wang, C. Qin and L. Dai, *Journal of Materials Science*, 2014, **49**, 3322.
16. B. Vigolo, A. Pénicaud, C. Coulon, C. Sauder, R. Pailler, C. Journet, P. Bernier and P. Poulin, *Science*, 2000, **290**, 1331.
17. A. J. Uddin, A. Watanabe, Y. Gotoh, T. Saito and M. Yumura, *Macromolecular Materials and Engineering*, 2012, **297**, 1114.
18. J. Liu, A. G. Rinzler, H. Dai, J. H. Hafner, R. K. Bradley, P. J. Boul, A. Lu, T. Iverson, K. Shelimov and C. B. Huffman, *Science*, 1998, **280**, 1253.
19. T. Saito, K. Matsushige and K. Tanaka, *Physica B: Condensed Matter*, 2002, **323**, 280.
20. N. Karousis, N. Tagmatarchis and D. Tasis, *Chemical Reviews*, 2010, **110**, 5366.
21. Y. Lin, B. Zhou, K. Shiral Fernando, P. Liu, L. F. Allard and Y.-P. Sun, *Macromolecules*, 2003, **36**, 7199.
22. T. S. Balaban, M. C. Balaban, S. Malik, F. Hennrich, R. Fischer, H. Rösner and M. M. Kappes, *Advanced Materials*, 2006, **18**, 2763.
23. C. Liebert, M. K. Brinks, A. G. Capacci, M. J. Fleming and M. Lautens, *Organic letters*, 2011, **13**, 3000.
24. N. A. Kumar, I. Jeon, G. Sohn, R. Jain, S. Kumar and J. Baek, *ACS nano*, 2011, **5**, 2324.
25. J. L. Bahr and J. M. Tour, *Journal of Materials Chemistry*, 2002, **12**, 1952.
26. X. Wu and P. Liu, *Express Polymer Letters*, 2010, **4**,723
27. J. Liu, *Science*, 1998, **280**, 1253.
28. A. Jorio, M. Pimenta, A. Souza Filho, R. Saito, G. Dresselhaus and M. Dresselhaus, *New Journal of Physics*, 2003, **5**, 139.
29. K. A. Wepasnick, B. A. Smith, J. L. Bitter and D. H. Fairbrother, *Analytical and bioanalytical chemistry*, 2010, **396**, 1003.
30. H. Murphy, P. Papakonstantinou and T. T. Okpalugo, *Journal of Vacuum Science & Technology B*, 2006, **24**, 715.
31. T. McNally, P. Pötschke, P. Halley, M. Murphy, D. Martin, S. E. Bell, G. P. Brennan, D. Bein, P. Lemoine and J. P. Quinn, *Polymer*, 2005, **46**, 8222.
32. D. Puglia, L. Valentini and J. Kenny, *Journal of applied polymer science*, 2003, **88**, 452.
33. L. Valentini, J. Biagiotti, J. Kenny and S. Santucci, *Composites Science and Technology*, 2003, **63**, 1149.
34. T. Terao, S. Maeda and A. Saika, *Macromolecules*, 1983, **16**, 1535.
35. M. Xu, Q. Huang, Q. Chen, P. Guo and Z. Sun, *Chemical Physics Letters*, 2003, **375**, 598.
36. Y. Hasegawa, Y. Inoue, K. Deguchi, S. Ohki, M. Tansho, T. Shimizu and K. Yazawa, *The Journal of Physical Chemistry B*, 2012, **116**, 1758.
37. M. Dionisio, J. M. Schnorr, V. K. Michaelis, R. G. Griffin, T. M. Swager and E. Dalcanale, *Journal of the American Chemical Society*, 2012, **134**, 6540.
38. J. Yu, B. Tonpheng, G. Gröbner and O. Andersson, *Macromolecules*, 2012, **45**, 2841.
39. L. Jiang, L. Gao and J. Sun, *Journal of Colloid and Interface Science*, 2003, **260**, 89.
40. A. Coats and J. Redfern, *Analyst*, 1963, **88**, 906.
41. R. K. Layek, S. Samanta and A. K. Nandi, *Carbon*, 2012, **50**, 815.
42. N. A. Peppas and E. W. Merrill, *Journal of Applied Polymer Science*, 1976, **20**, 1457.
43. X. Zhang, X. Fan, H. Li and C. Yan, *Journal of Materials Chemistry*, 2012, **22**, 24081.

MWCNTs dispersion was improved by grafting PVA through Friedel-Crafts alkylation and thus mechanical properties of PVA/MWCNTs fibers were increased